Interactions of the Inactivation Peptide with the R State

To investigate the interactions of the inactivation peptide with the R state during channel recovery, we subjected channels to a double pulse protocol (Fig. S1). Cells expressing WT Kv1.5 or Kv1.4N/Kv1.5 were pulsed to +60 mV for 800 ms and repolarized to −100 mV for 100 ms, followed by a second depolarization to +60 mV. In WT Kv1.5, the second depolarizing pulse elicits an outward current that decays much more slowly than the first (Fig. S1 A). We have previously demonstrated that this current decay is governed by the transition from the R state to the C-type–inactivated state (Scheme I) (Wang, Z.R., J.C. Hesketh, and D. Fedida. 2000. *Biophys. J.* 79:2416–2433). In the Kv1.4N/Kv1.5 chimera, with intact N-type inactivation, the current decay in the second pulse is more rapid (Fig. SI1B). To illustrate this observation more clearly, currents from the second depolarizing pulse have been normalized and magnified in Fig. S1 C. These data demonstrate that the presence of the inactivation peptide increases the decay rate of currents through the R state, suggesting that the inactivation peptide can bind to the R state and block currents through this state.

A recent report (Jiang, X., G.C. Bett, X. Li, V.E. Bondarenko, and R.L. Rasmusson. 2003. *J. Physiol.* 549:683–695) has suggested that C-type inactivation involves a significant constriction of the inner mouth of the channel pore, leading to inner pore dimensions similar to those of deactivated channels. This finding raises the possibility that the rising phase of the slow Na^+ tail is due to a rearrangement/reopening of the inner pore, and also suggests that the onset of C-type inactivation might result in occlusion of the inactivation peptide from the pore. This possibility is summarized by the state diagram in Scheme SI, in which the inactivation peptide is surmised to bind to the

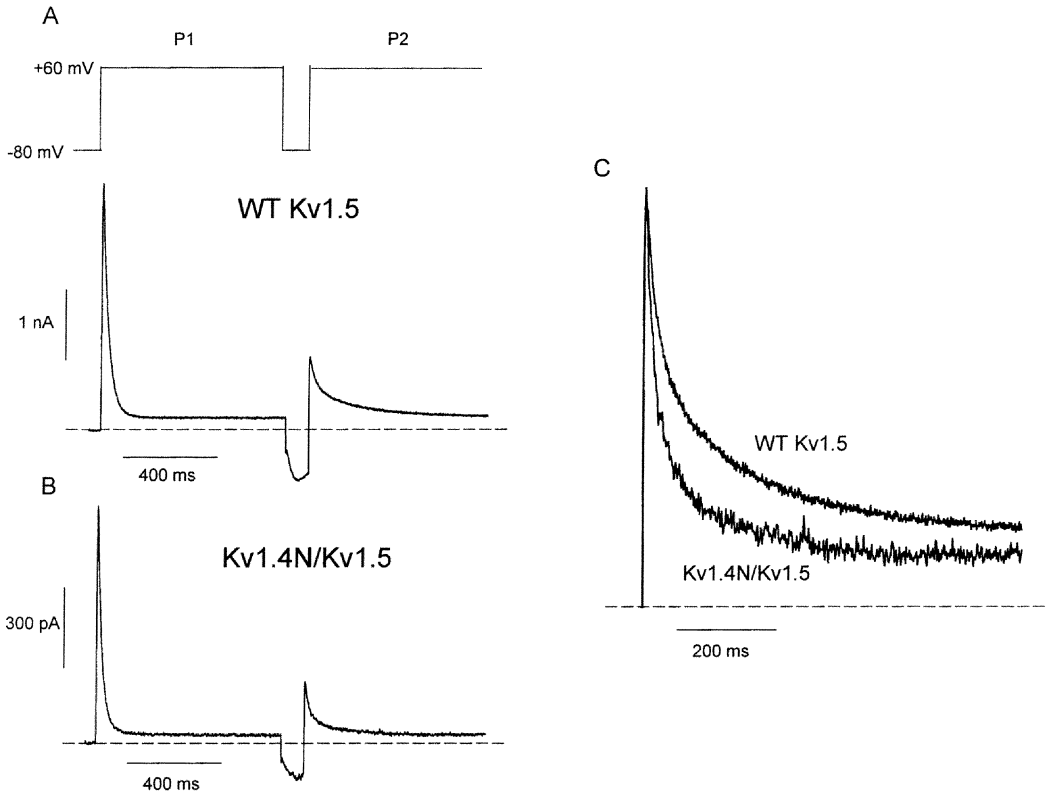

Figure S1. Interactions between the R-state and the inactivation peptide. Cells were subjected to a double pulse protocol to elicit currents through the R state. From a holding potential of −80 mV, cells expressing (A) WT Kv1.5 or (B) Kv1.4N/Kv1.5 were pulsed to +60 mV for 800 ms (P1) and repolarized to −100 mV for 100 ms, followed by a second depolarization to +60 mV (P2). (C) The currents elicited during the second depolarizing pulse (P2) have been normalized and magnified, to illustrate the accelerated current decay in Kv1.4N/Kv1.5.

highly Na^+-permeable R state, but is excluded from binding to the pore of C-type–inactivated channels.

We found Scheme SI difficult to reconcile with our experimental results for several reasons. Firstly, if the inner pore reopens during recovery from inactivation, and thereby exposes a binding site for the inactivation peptide/QA compounds, this model predicts a reduction in the delay of the peak tail current. However, our experimental data clearly show an increased delay of the peak tail current in the presence of the inactivation peptide (see Fig. 5 in main text). This model also cannot account for the clear time dependence of tail current slowing observed in Kv1.4 (see Fig. 5 A), where the inactivation peptide and quaternary ammonium ions clearly appear to bind the C-type inactivated state.

The experimental data in Fig. S1 suggest a more complete version of our final model. This is depicted in Scheme SII, in which the inactivation peptide is also permitted to bind the R state during recovery from inactivation. This is likely more correct than the scheme in Fig. 8 A, for two reasons. First, the activation gates are very likely open in the R state, otherwise ions would be occluded from the permeation pathway, and no Na^+ tail would be apparent. The open activation gate leaves the inner vestibule cytosolically accessible, exposing the binding site for the inactivation peptide. Secondly, Scheme SII accounts for the results of the double pulse experiment, which suggests an interaction between the inactivation peptide and the R state.

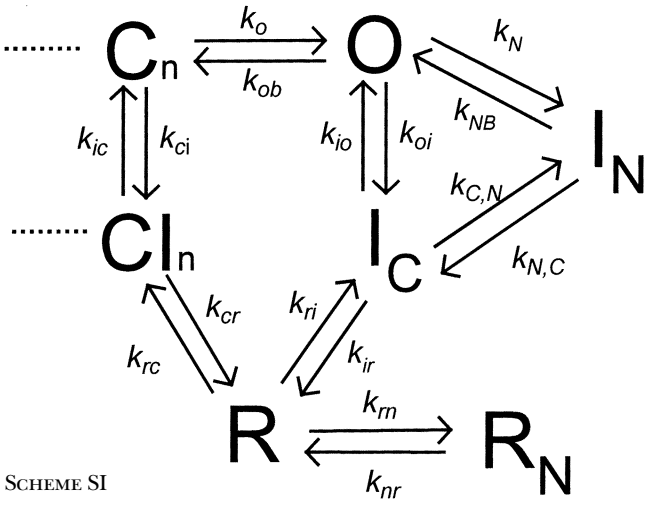

SCHEME SI

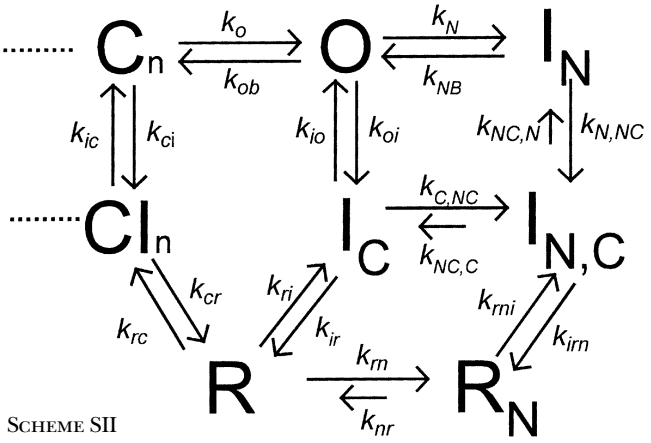

SCHEME SII